Interaction of Nucleotides with Acidic Fibroblast Growth Factor (FGF-1)

Ashok J. Chavan* and Boyd E. Haley

College of Pharmacy, Lucille P. Markey Cancer Center, University of Kentucky, Lexington, Kentucky 40536

David B. Volkin, Kimberly E. Marfia, Adeline M. Verticelli, Mark W. Bruner, Jerome P. Draper, Carl J. Burke, and C. Russell Middaugh*

Department of Pharmaceutical Research, Merck Research Laboratories, WP78-302, West Point, Pennsylvania 19486

Received November 22, 1993; Revised Manuscript Received April 15, 1994®

ABSTRACT: A wide variety of nucleotides are shown to bind to acidic fibroblast growth factor (aFGF) as demonstrated by their ability to (1) inhibit the heat-induced aggregation of the protein, (2) enhance the thermal stability of aFGF as monitored by both intrinsic fluorescence and CD, (3) interact with fluorescent nucleotides and displace a bound polysulfated naphthylurea compound, suramin, (4) reduce the size of heparin–aFGF complexes, and (5) protect a reactive aFGF thiol group. The binding of mononucleotides, diadenosine compounds (Ap_nA), and inorganic polyphosphates to aFGF is enhanced as the degree of phosphorylation of these anions is increased with the presence of the base reducing the apparent binding affinity. The nature of the base appears to have much less effect. Photoactivatable nucleotides ($8N_3$-ATP, $2N_3$-ATP, $8N_3$-GTP, and $8N_3$-Ap_4A) were employed to covalently label the aFGF nucleotide binding site. In general, K_d's in the low micromolar range are observed. Protection against 90% displacement is observed at several hundred micromolar nucleotide concentration. Using $8N_3$-ATP as a prototypic reagent, photolabeled aFGF was proteolyzed with trypsin and chymotrypsin and labeled peptides were isolated and sequenced resulting in the identification of 10 possible labeled amino acids (Y8, G20, H21, T61, K112, K113, S116, R119, R122, H124). On the basis of the crystal structure of bovine aFGF, eight of the prospective labeled sites appear to be dispersed around the perimeter of the growth factor's presumptive polyanion binding site. One residue (T61) is more distally located but still proximate to several positively charged residues, and another (Y8) is not locatable in crystal structures. Using heparin affinity chromatography, at least three distinct photolabeled aFGF species were resolved. These labeled complexes display diminished affinity for heparin and a reduced ability to stimulate mitogenesis even in the presence of polyanions such as heparin. In conclusion, nucleotides bind apparently nonspecifically to the polyanion binding site of aFGF but nevertheless are capable of modulating the protein's activity. Evidence for the presence of a second or more extended polyanion binding site and the potential biological significance of these results in terms of potential natural ligands of aFGF are also discussed but not resolved.

Acidic fibroblast growth factor (aFGF; FGF-1),[1] one of the prototypic members of the fibroblast growth factor family, is a relatively labile protein manifesting significant structural disruption at physiological temperatures (Copeland et al., 1991; Dabora et al., 1991). The protein is dramatically stabilized, however, by the binding of polyanions such as heparin. Interaction of aFGF with naturally occurring anionic extracellular matrix macromolecules such as heparan sulfate has been posulated to protect the protein in its biological milieu where it can be released in an active form by enzymatic processes (Vlodavsky et al., 1991). Recent evidence suggests that the receptor competent form of the FGFs is an FGF/polyanion complex in which the polyanion may mediate oligomerization (e.g., dimerization) of high-affinity FGF receptors, an early signal transduction event (Ornitz et al., 1992).

The structural requirements for polyanion binding to aFGF are remarkably nonspecific *in vitro* with macromolecular polyanionic molecules as diverse as polysaccharides, polypeptides, and polynucleotides as well as various small highly sulfated and phosphorylated molecules all able to stabilize the protein (Tsai et al., 1993; Volkin et al., 1993). An initial identification of the polyanion binding site has been made from complementary studies of several different FGFs employing a combination of chemical and crystallographic methods (Volkin et al., 1993; Zhu et al., 1993). This region appears to be formed primarily by a group of tightly clustered basic residues on the surface of the growth factors, although the extent of this site remains to be better defined.

Several small, highly phosphorylated compounds exist at sufficiently high concentrations within cells that they could potentially interact with and stabilize aFGF. For example, both the highly phosphorylated inositols (e.g., inositol tetra-, penta- and hexaphosphate) (Bunce et al., 1993; Guse et al., 1993; Menniti et al., 1993) and the nucleotide polyphosphates (e.g., ATP, GTP) (Lehninger, 1982) are present at micromolar to millimolar levels and undergo large concentration changes in response to various physiological stimuli. Thus, regulation of the activity of aFGF could possibly occur through the binding of such compounds. Both of these classes of polyanions have, in fact, been shown to bind and stabilize aFGF (Tsai et al., 1993; Volkin et al., 1993). Interestingly, the binding of polyanions to aFGF has been shown to prevent its passage into cells when diphtheria toxin is employed as a vector

* Authors to whom correspondence should be addressed.

® Abstract published in *Advance ACS Abstracts,* May 15, 1994.

[1] Abbreviations: aFGF, acidic fibroblast growth factor; ATeP, adenosine 5′-tetraphosphate; Ap_nA, diadenosine mono-, di-, tri-, tetra-, penta-, hexaphosphate in which n = 1, 2, 3, 4, 5, 6, respectively; TNP-ATP, (trinitrophenyl)adenosine 5′-triphosphate; N_3-ATP, azidoadenosine 5′-triphosphate; N_3-GTP, azidoguanosine 5′-triphosphate; N_3-Ap_4A, azidoadenosine 5′,5‴-tetraphosphate adenosine; DTNB, 5,5′-dithiobis-(2-nitrobenzoic acid); PCA, perchloric acid.

0006-2960/94/0433-7193$04.50/0

(Wiedlocha et al., 1992). In this case, interaction with anions probably inhibits the formation of molten globule forms of aFGF which could be translocation competent species (Mach et al., 1993a).

Therefore, to further explore the nature of the polyanion binding site of aFGF, we have characterized the interaction of nucleotides with this protein in greater detail. In addition, we have taken advantage of the availability of photoactivatible forms of several phosphorylated nucleotides to identify aFGF residues at or near the nucleotide binding site. This approach has been successfully employed to identify nucleotide binding sites on a large number of different proteins (Haley, 1991; Chavan et al., 1992; Salvucci et al., 1992).

MATERIALS AND METHODS

Materials

Polyphosphates as well as the phosphorylated nucleotides and dinucleotides were purchased from Sigma. Heparin was obtained from Hepar, sucrose octasulfate from Toronto Research Chemicals, and suramin from Mobay Chemical. Other reagents were purchased commercially and were of the highest grade available.

The recombinant human aFGF (15.9 kDa) utilized in this study, an amino terminal truncated, 141 amino acid residue form, was expressed in transformed *Escherichia coli* cells as previously described (Copeland et al., 1991). The protein was purified by a combination of ion-exchange and affinity chromatography as described elsewhere (Volkin et al., 1993). The purified, unliganded protein was stored at −70 °C in a phosphate-buffered saline solution (PBS) containing sodium sulfate and EDTA for stability enhancement (Tsai et al., 1993). Samples of unliganded protein were thawed, stored on ice, and examined on the same day.

Methods

Turbidity Measurements. The rate of protein aggregate formation at 40 °C was followed by monitoring the degree of light scattering at 350 nm using a Perkin-Elmer Lambda 6 spectrophotometer equipped with a thermojacketed cuvette holder as described in detail elsewhere (Tsai et al., 1993; Volkin et al., 1993). Experiments were performed with 1.0-mL samples of 100 μg/mL aFGF in PBS buffer containing the indicated amounts of various polyanionic ligands.

Circular Dichroism. CD spectra were measured with an Aviv 62DS spectropolarimeter. Samples of aFGF at 100 μg/mL in PBS buffer containing various amounts of phosphorylated ligands were placed into 1 mm path length cells with the cell temperature controlled by a Peltier device. To monitor thermal unfolding, the change in ellipticity at 228 nm as a function of temperature was measured as described previously (Burke et al., 1993; Volkin et al., 1993).

Fluorescence Measurements. Fluorescence spectra were measured with either a Hitachi F-4500 or a Spex Fluorolog fluorometer at 4- or 10-nm resolutions employing excitation at 280 nm. Thermal melting experiments with 100 μg/mL aFGF in a PBS buffer containing the indicated amounts of various polyanions were performed with the Spex instrument as described elsewhere (Copeland et al., 1991; Volkin et al., 1993).

Protection of aFGF Thiol Groups by Polyanions. The rate of reaction of 0.2 mM DTNB (Ellman's reagent) with aFGF (100 μg/mL in a PBS buffer in the presence and absence of 0.5 mM polyanionic ligands) was determined by monitoring color formation at 412 nm over time at 10 °C with a Hitachi U3210 spectrophotometer. Measurements with unliganded aFGF showed the expected 3.0 (±0.3) mol of cysteine residues/mol of protein after the reaction rate leveled off after approximately 30 min.

Heparin Affinity Chromatography. Photolabeled aFGF was eluted from a 5 × 0.5 cm TosoHaas heparin affinity column at 0.5 mL/min employing a 40-min 0–1.5 M linear NaCl gradient. Elution was monitored at 215 and 280 nm. To isolate sufficient quantities of protein for spectral and mitogenic analysis, multiple injections of 200 μL (50 μg of protein) were performed, and each of the three major peaks was combined and concentrated by centrifugal ultrafiltration. Protein concentrations were determined by the Micro BCA method (Pierce). The identity of each peak as a form of photolabeled aFGF was supported by both SDS–PAGE and gel filtration experiments in which each peak from the heparin affinity column was observed to contain a single species with an apparent molecular weight slightly greater than that of unlabeled protein.

Mitogenic Activity. The biological activity of aFGF in the presence or absence of various polyanionic compounds (0.5 mg/mL in the tissue culture medium) was monitored as the mitogenic response of Balb/c3T3 cell lines as determined by uptake of tritiated thymidine (Linemeyer et al., 1987).

Light Scattering. Light-scattering experiments utilized a Malvern 4700 spectrometer (Malvern, England) equipped with a 5-W argon laser (Spectra Physics). The preparation of aFGF–heparin complexes and the analysis of static light scattering data to measure the competitive binding of various polyanionic ligands to aFGF–heparin complexes has been described elsewhere (Mach et al., 1993b).

Suramin Fluorescence. The suramin–aFGF complex was prepared as described previously (Middaugh et al., 1992) and excited at 315 nm in a Hitachi F-2000 fluorometer with emission monitored from 340 to 540 nm. The enhancement of suramin fluorescence by aFGF and the subsequent decrease in this enhancement of suramin fluorescence produced by the addition of polyanionic ligands has been described previously (Middaugh et al., 1992).

(TNP-ATP)/aFGF Interactions. The enhancement of TNP-ATP fluorescence in the presence of aFGF was monitored in a Hitachi F-4500 fluorometer with excitation at 408 nm. TNP-ATP was prepared at 30 μM in a PBS buffer at 10 °C with varying amounts of aFGF (0–150 μM). After a 10-min incubation, fluorescence spectra were collected. The ability of polyanions to disrupt TNP-ATP–aFGF complexes was determined by incubating a 1:1 ratio of protein and ligand (25 μM) with varying amounts of either heparin or sucrose octasulfate for 10 min at 10 °C before collecting fluorescence spectra.

Synthesis of Photoprobes. The nucleotide photoaffinity probes [α- or γ-^{32}P]-8N_3-ATP, [γ-^{32}P]-2N_3-ATP, [γ-^{32}P]-8N_3-GTP, and [β-^{32}P]-8N_3-Ap_4A were synthesized by methods previously described (Michelson, 1964; Czarnecki et al., 1979; Salvucci et al., 1992).

Photoaffinity Labeling. aFGF (1.0 μg) in 30 μL of 10 mM Tris, pH 7.0 (photolysis buffer), was incubated with various concentrations of probe at 4 °C for 30 s and photolyzed at 4 °C for 30 s with a hand-held UV lamp with the filter removed (6000 μW/cm^2). The reaction was quenched by addition of a protein solubilizing mixture containing 10% SDS, 3.6 M urea, 162 mM DTT, pyronin Y (tracking dye), and 20 mM Tris, pH 8.0. The samples were separated by 12% SDS–PAGE, stained by Coomassie Brilliant Blue R, destained, dried on a slab gel dryer, and exposed to X-ray film (Cronex

DuPont). The individual protein bands were excised, and the radioactivity was determined by liquid scintillation counting.

For protection experiments, aFGF (1.0 μg) in 30 μL of photolysis buffer was initially incubated with varying concentrations of competitors at 4 °C for 1 min followed by 10 μM probe at 4 °C for 30 s and photolyzed at 4 °C for 30 s. The samples were analyzed as described above.

Isolation of [γ-^{32}P]-8N$_3$-ATP Photolabeled Tryptic Peptides of aFGF. In a plastic weighing boat, aFGF (500 μg) was incubated with probe (probe to protein molar ratio of 5:1) in a final volume of 1.9 mL of 10 mM Tris, pH 7.0, at 4 °C for 1 min, photolyzed at 4 °C for 1.5 min, followed by a second incubation with probe (probe to protein molar ratio of 5:1) in a final volume of 2.0 mL of buffer, and photolyzed. The photolabeled aFGF was precipitated by adding an equal volume of ice-cold 7% PCA. The pellet was resuspended in 1.0 mL of 100 mM NH_4HCO_3 containing 2 M urea and digested with 4% (w/w) modified trypsin for 3 h followed by a second addition of 4% (w/w) trypsin and incubation at 25 °C for 14 h.

Immobilized Al^{3+} Chromatography. The resin (1.5 mL) was prepared for chromatography (Chavan et al., 1992; Salvucci et al., 1992; Shoemaker & Haley, 1993) by washing successively with 20 mL of water, 20 mL of 50 mM $AlCl_3$, 10 mL of water, and 20 mL of 100 mM ammonium acetate, pH 5.9 (buffer A). The digested aFGF was diluted with buffer A and (a) loaded onto the resin, (b) washed with buffer A, (c) washed with buffer A containing 0.5 M NaCl, (d) washed with buffer A, and (e) washed with buffer A containing 10 mM K_2HPO_4, pH 8.0. The radioactivity in collected fractions (~1.5 mL) was determined by Cerenkov counting.

Reverse Phase HPLC Purification of Photolabeled Peptides Purified by Immobilized Al^{3+} Chromatography. The radioactive fractions eluted by the phosphate wash from the Al^{3+} resin were pooled, concentrated, and purified by reverse phase HPLC on an Aquapore RP300 C8 column using a gradient of 0% B at 0–5 min and 100% B at 65 min at 0.5 mL/min (solvent A, 0.1% TFA; solvent B, 70% acetonitrile, 0.1% TFA). The radioactivity in the fractions collected (0.5 mL) was determined by Cerenkov counting. Radioactive fractions showing corresponding absorbance at 214 nm were subjected to amino acid sequence analysis on an Applied Biosystems 477A protein sequenator at University of Kentucky Macromolecular Facility.

Isolation of [γ-^{32}P]-8N$_3$-ATP Photolabeled Chymotryptic Peptides of aFGF. aFGF (500 μg) was photolabeled, and the unbound probe was removed by PCA precipitation as described above. The pellet was resuspended in 1.1 mL of 100 mM NH_4HCO_3 containing 2 M urea and digested with 2% (w/w) chymotrypsin for 2 h followed by a second addition of 2% (w/w) chymotrypsin and incubation at 25 °C for 14 h. Immobilized Al^{3+} chromatography was performed as described previously. The photolabeled peptides were eluted first with buffer A containing 10 mM K_2HPO_4, pH 5.9, followed by buffer A containing 10 mM K_2HPO_4, pH 8.0. The phosphate washes from the Al^{3+} resin were pooled, concentrated, and purified by reverse phase HPLC also as described above. The radioactive fractions obtained at 33 and 34 min were pooled, concentrated, and repurified on an Aquapore RP300 C8 column using a gradient of 0% B at 0–5 min and 85% B at 65 min at 0.5 mL/min. The radioactive fraction obtained at 37 min was subjected to amino acid sequence analysis.

Molecular Modeling. Crystallographic coordinates of bovine aFGF lacking the N-terminal decapeptide were provided by Drs. Doug Rees and Barbara Hsu (personal communication) (Zhu et al., 1991). The structure was rendered using Quanta software on a Silicon Graphics Indigo workstation. Residues unique to the bovine form were replaced with the residues found in human aFGF (Volkin et al., 1993). The 10 amino acids were located on or near the surface of the protein, thus minimizing potential perturbations of the backbone. After energy minimization using CHARMM, no significant changes were observed in the backbone conformation of the protein.

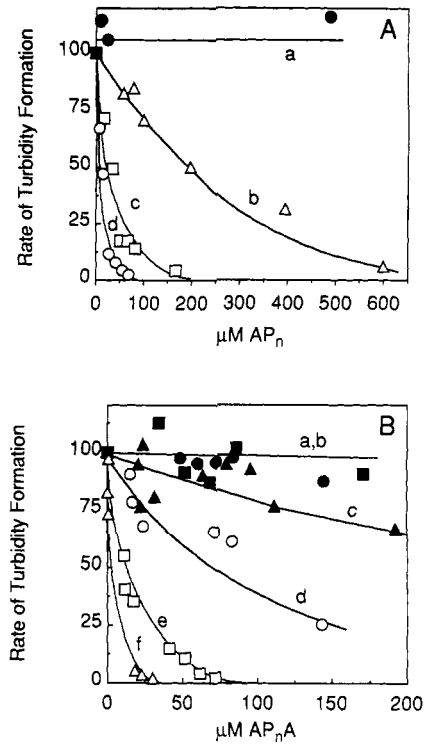

FIGURE 1: Effect of nucleotides on the temperature-induced aggregation of aFGF. The rate of turbidity formation at 40 °C was monitored at 350 nm and is expressed in relative units. All solutions contained 100 μg/mL aFGF in 6 mM sodium phosphate, 120 mM NaCl, pH 7.2, and the indicated concentration of nucleotide: (A) (a) AMP, (b) ADP, (c) ATP, (d) ATeP, (B) (a) ApA, (b) Ap$_2$A, (c) Ap$_3$A, (d) Ap$_4$A, (e) Ap$_5$A, (f) Ap$_6$A.

RESULTS

Stabilization of aFGF by Nucleotides

The stabilization of aFGF produced by the binding of anions provides a convenient basis with which to detect such interactions. For example, at 40 °C the structure of the protein is perturbed and it begins to aggregate, producing measurable increases in light scattering (Tsai et al., 1993; Volkin et al., 1993). Using the initial rate of turbidity formation at 350 nm as a measure of aFGF instability, the effect of adenosine nucleotides was examined (Figure 1A). While AMP had no detectable effect on the heat-induced aggregation of aFGF, more highly phosphorylated forms of adenosine inhibited aggregation in the order of effectiveness ATeP (10 μM) > ATP (30 μM) > ADP (200 μM); the numbers shown in parentheses are the concentrations of nucleotide necessary to inhibit the rate of aggregation by 50% (IC_{50}). These concentrations correspond to a molar excess of nucleotide to protein of approximately 1.5, 5, and 33, respectively.

A similar tendency is seen with variably phosphorylated diadenosine compounds (Figure 1B). The mono- and diphosphorylated forms of diadenosine (ApA and Ap$_2$A) have little effect on aFGF stability, but more phosphorylated species

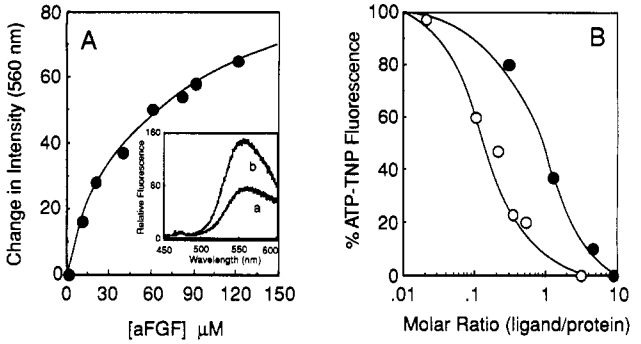

FIGURE 2: (A) Effect of aFGF on the fluorescence of TNP-ATP. The fluorescent nucleotide analog was excited at 408 nm and was present at a concentration of 30 μM. The inset shows the effect of 120 μM aFGF (b) on the emission spectrum of TNP-ATP (30 μM) while the less intense spectrum in the absence of the protein is illustrated in spectrum a. (B) Competition by heparin (○) and sucrose octasulfate (●) for the binding of TNP-ATP to aFGF as monitored by the decrease in fluorescence of the nucleotide analogue. Conditions are the same as those in part A.

inhibit aFGF aggregation in the order Ap_6A (3 μM) > Ap_5A (10 μM) > Ap_4A (30 μM) > Ap_3A (250 μM). As above, the parenthetical values are the concentrations of ligands producing 50% inhibition, which correspond to Ap_nA/aFGF molar ratios of 0.5, 1.5, 5, and 42, respectively. These values can be compared to the IC_{50} values of 6 mM and 7 μM for phosphate and tetrapolyphosphate, respectively (ligand:aFGF = 1000:1 and 1.2:1) (not illustrated).

To more directly establish the binding of ATP to aFGF, the interaction of the fluorescent probe TNP-ATP with the growth factor was characterized. In the absence of aFGF, the fluorescence maximum of TNP-ATP is observed near 560 nm. Upon addition of increasing amounts of aFGF to 30 μM TNP-ATP, the spectrum of the weakly fluorescent TNP-ATP undergoes a gradual increase in fluorescence intensity and shift to lower wavelengths (Figure 2A). These spectral changes saturate at a 2-fold intensity increase and 5-nm blue shift, with the midpoint occurring at approximately 30 μM aFGF. The addition of approximately equimolar amounts of sucrose octasulfate and 1/10 of multivalent 16-kDa heparin is required for complete return of the TNP-ATP spectral parameters to their unbound values (Figure 2B).

The binding of ATP to aFGF could also be demonstrated by competition with the fluorescent polyanion suramin, a polysulfated naphthylurea. This compound has previously been shown to bind to the polyanion binding site of aFGF with a concomitant increase in its fluorescence emission intensity (Middaugh et al., 1992). When ATP is added to a solution of suramin-complexed aFGF, the fluorescence of the suramin is decreased to 50% that of the complex at approximately a 1000-fold excess of the nucleotide triphosphate (Figure 3). Other polyphosphates mentioned in this study such as tetrapolyphosphate also showed similar competition although with enhanced affinity compared to ATP (not illustrated).

As a measure of relative affinity, ATP was compared to the known high-affinity ligand, heparin. To this end, we examined the ability of ATP to decrease the size of aFGF–heparin complexes as detected by a reduction in the intensity of the light scattered by these entities. A molecule of 16-kDa heparin possesses the ability to bind 10–15 molecules of aFGF (Mach et al., 1993b). When ATP is added to a heparin chain saturated with aFGF (which is responsible for the majority of the light scattered by the complex), the scattering intensity decreases, although in this case, over a 10000-fold molar excess

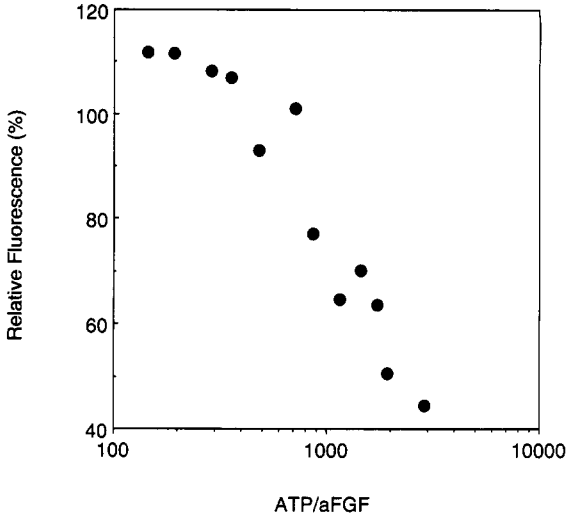

FIGURE 3: Effect of ATP on the fluorescence of suramin in the presence of aFGF. Suramin was excited at 315 nm and its fluorescence monitored at 403 nm. Suramin and the protein were present at concentrations of 10 and 6 μM, respectively.

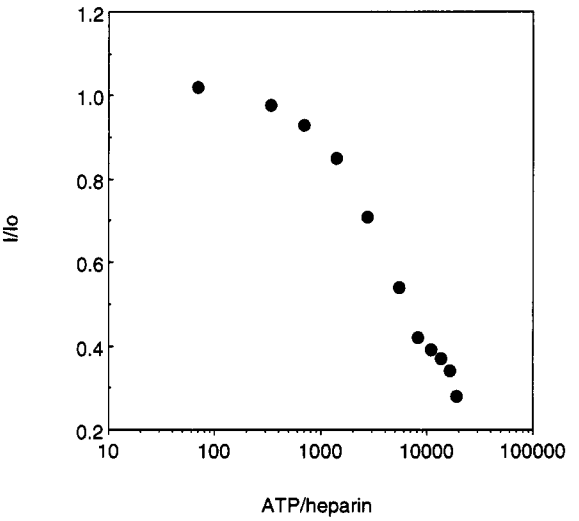

FIGURE 4: Effect of ATP on the size of aFGF–heparin complexes as monitored by the light scattering intensity in the presence (I) and absence (I_0) of ATP. Measurements were made at a protein concentration of 62 μM at 10 °C and a 90° scattering angle.

of ATP is necessary to reduce scattering to that of an uncomplexed mixture of aFGF and heparin (Figure 4). Similar results were obtained with tetrapolyphosphate (not illustrated), although lesser quantities of this compound were required.

The effect of various polyphosphorylated compounds on the thermal stability of aFGF was also examined. In these experiments, the structure of aFGF was monitored by a combination of fluorescence and CD spectroscopy. When aFGF is structurally disrupted, the fluorescence of its single quenched tryptophan residue is dramatically enhanced, providing a sensitive measure of tertiary structure integrity (Copeland et al., 1991). More extensive alteration of the protein produces changes in the far-UV CD of the protein due primarily to unfolding of secondary structure. Thermally induced changes in the structure of aFGF are first seen in intrinsic fluorescence changes as temperature is increased. These are followed at somewhat higher temperatures ($\Delta T \sim$ 5–20 °C) by secondary structure loss. These two phenomena are not tightly coupled in the case of aFGF and are thought to reflect the formation of a molten globule state between the

Table 1: Thermal Unfolding Temperature of aFGF in the Presence of Various Phosphorylated Compounds As Determined by Both Fluorescence Spectroscopy and CD[a]

aFGF soln containing	T_m (°C) fluorescence[b]	T_m (°C) CD[c]
0.6 mM PO_4 buffer	26	39
6 mM PO_4 buffer + 200 mM NaCl	36	50
6 mM PO_4 buffer	37	47
100 mM PO_4 buffer	45	56
trimeta PO_4 (ring) (0.5 mM)	38	50
inorganic Pyro PO_4 (0.5 mM)	44	52
tripoly PO_4 (chain) (0.5 mM)	48	58
tetrapoly PO_4 (0.5 mM)	48	62
AMP (0.5 mM)	40	49
ATP (0.5 mM) + 0.6 mM PO_4	42	48
ADP (0.5 mM)	42	50
deoxy ATP (0.5 mM)	46	53
ATP (0.5 mM)	47	53
ATeP (0.5 mM)	53	58
CTP (0.5 mM)	46	55
TTP (0.5 mM)	46	54
GTP (0.5 mM)	49	54
ApA (0.5 mM)	41	48
Ap_2A (0.5 mM)	41	49
Ap_3A (0.5 mM)	41	49
Ap_4A (0.5 mM)	44	52
Ap_5A (0.5 mM)	51	60
Ap_6A (0.5 mM)	52	60
$pd(A)_{14}$ (0.5 mM)	38	46

[a] Samples contained 100 μg/mL protein in 6 mM phosphate buffer and 120 mM NaCl (unless otherwise stated) and the indicated amount of polyanion. [b] Midpoint of the thermally induced intrinsic fluorescence transition obtained by monitoring the wavelength of maximum emission. All values are ±1 °C. [c] Midpoint of the thermally induced CD transition obtained by measurement of the ratio of the ellipticities at 228 and 250 nm. All values are ±1 °C.

two events (Mach et al., 1993a). The results of measurements of these thermal disruption temperatures by both methods are summarized in Table 1 for a variety of phosphorylated polyanions.

In dilute (0.6 mM) phosphate buffer, aFGF is relatively unstable, with the midpoints of its thermal transitions detected by fluorescence and CD observed at 26 and 39 °C, respectively. A 10-fold increase in phosphate concentration (6 mM) produces a ca. 10 °C increase in both T_m's. Addition of 200 mM NaCl has little additional effect, but the presence of 100 mM phosphate causes another 8–9 °C increase in stability. Polyphosphates and nucleotides were all tested at 0.5 mM, a concentration at which the most potent compounds saturated their effect. A very similar trend was seen in all three of the major classes of agents examined: increases in the extent of phosphorylation are accompanied by a corresponding enhancement in the ability of polyphosphate, adenosine nucleotides, and diadenosine compounds to stabilize aFGF. Several additional observations seem warranted: (1) the linear form of tripolyphosphate is much more effective than the cyclic form; (2) the nature of the base in the nucleotide triphosphates seems to have only minor effects on the ability of the compounds to stabilize aFGF; (3) in general, the presence of the base appears to moderately reduce the effectiveness of the nucleotides as seen by comparing the adenosine nucleotides and diadenosines to corresponding polyphosphates if the sensitivity of the secondary structure sensitive CD signal is employed as a criterion; (4) the stabilizing effect of the phosphates seems to saturate in each class of compounds at the level of the triphosphate in the polyphosphates, the tetraphosphate in the adenosine nucleotides, and the pentaphosphate in the adenosine dinucleotides; (5) spacing the phosphate groups (i.e., $pd(A)_{14}$) dramatically reduces their effectiveness; (6) modification of the sugar (deoxy ATP) has no detectable effect; (7) the difference in the two T_m values (CD and fluorescence) for each class of compounds seems relatively invariant, except for the linear polyphosphates in which the difference in thermal unfolding temperature seems slightly greater.

It has previously been shown that aFGF contains a reduced thiol moiety in the vicinity of its polyanion binding site whose reactivity with thiol specific reagents is protected by the presence of polyanions (Volkin et al., 1993). We therefore also examined the effect of several of the polyanions of this study on rate of reaction of this thiol group with DTNB at the ligand concentration used in the stability studies (0.5 mM) (results not illustrated). Heparin and tetrapolyphosphate dramatically reduce this reaction rate by a factor of greater than 200-fold. Somewhat lesser protective effects were seen with Ap_5A (45×) and ATP (5×), although both nucleotides still markedly reduced the rate of reaction of aFGF with DTNB compared to unliganded protein. The ability of representative examples of the polyanions indicated in Table 1 to stimulate mitogenic activity was also examined (not illustrated). When 0.5 g/L polyanion was employed in the tissue culture medium, inositol hexaphosphate and tetrapolyphosphate were found to enhance the ability of aFGF to stimulate the uptake of tritiated thymidine into 3T3 cells by approximately 20-fold, an extent similar but not equivalent to that produced by heparin. In contrast, the two nucleotides tested, ATP and Ap_5A, were ineffective since in their presence mitogenic activity was similar to that observed in the absence of polyanions.

Photolabeling of aFGF with Azido Nucleotides

The availability of photoactivable azido nucleotides suggested that these compounds might be used to identify residues in the vicinity of the aFGF polyanion binding site. The ability of ^{32}P-labeled $8N_3$-ATP, $2N_3$-ATP, $8N_3$-GTP, and $8N_3$-Ap_4A to photolabel aFGF was therefore examined. Less phosphorylated analogues labeled aFGF much less efficiently. The effect of [α-^{32}P]-$8N_3$-ATP concentration on photoincorporation into aFGF is shown in Figure 5A. Photolabeling saturates at approximately 5–7 μM nucleotide with an apparent K_d of 2–2.5 μM. A minimum of 9% of the protein was labeled under these conditions with a pH optimum of 7.5 (in Tris buffer). Both phosphate and sulfate ions were found to inhibit labeling as expected (not illustrated). Ninety percent protection from this labeling was achieved by 200 μM ATP (Figure 5B). These results as well as those obtained for $2N_3$-ATP, $8N_3$-GTP, and $8N_3$-Ap_4A are summarized in Table 2. Both $8N_3$-GTP and $8N_3$-Ap_4A label aFGF with efficiencies similar to that of $8N_3$-ATP, but $2N_3$-ATP is significantly less efficient, with a 15–20-fold increase in apparent K_d and reduction in the amount of protein labeled.

The specificity of the nucleotide photoaffinity labeling of aFGF was examined in more detail for $8N_3$-ATP and $8N_3$-GTP (Figure 6A,B). In these experiments, a 5 μM concentration of the azido nucleotide was incubated with 100 μM concentrations of each agent. In both cases, the various nucleotide triphosphates examined (ATP, GTP, CTP, UTP) inhibited photolabeling to a similar extent in agreement with the stabilization studies (Table 1). Nucleotide di- and monophosphates were decreasingly effective, respectively. The tetraphosphorylated diadenosine compound was similar in potency to the nucleotide triphosphate. Most effective of all, however, at blocking photoincorporation were the non-nucleotide sulfated polyanions heparin and suramin, which

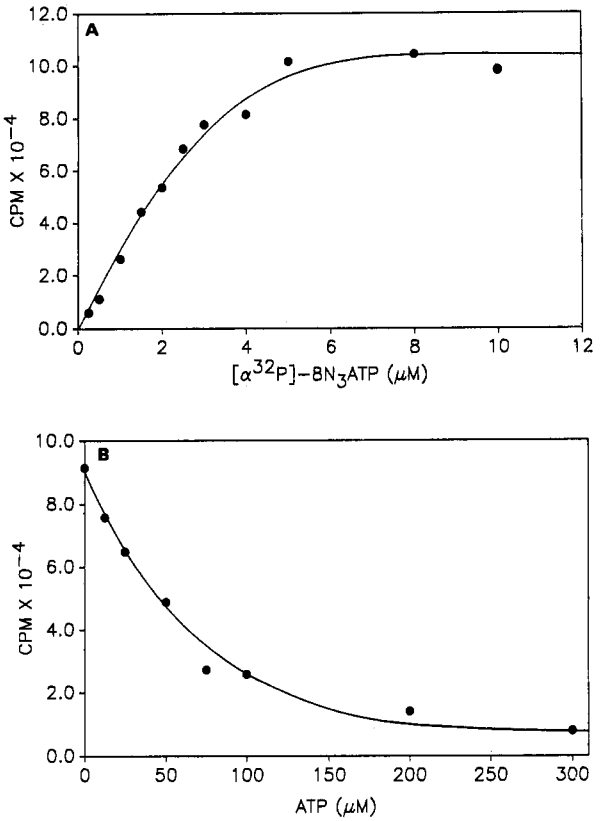

FIGURE 5: (A) Saturation of photoinsertion of [α-^{32}P]-8N$_3$-ATP into aFGF. aFGF (1.0 μg) in 30 μL of 10 mM Tris, pH 7.0 (photolysis buffer), was incubated with increasing concentrations of probe (sp. act 8.14 mCi/μmol) at 4 °C for 30 s and photolyzed at 4 °C for 30 s with a hand-held UV lamp with filter removed (6000 μW/cm^2). The reaction was quenched by addition of a protein solubilizing mixture. The samples were separated by 12% SDS–PAGE, stained by Coomassie Brilliant Blue R, destained, dried on a slab gel dryer, and exposed to X-ray film (Cronex DuPont). The individual protein bands were excised, and the radioactivity was determined by liquid scintillation counting. (B) Protection of photoinsertion of [γ-^{32}P]-8N$_3$-ATP in aFGF by ATP. aFGF (1.0 μg) in 30 μL of photolysis buffer was initially incubated with varying concentrations of ATP at 4 °C for 1 min followed by 10 μM probe at 4 °C for 30 s and photolysis at 4 °C for 30 s. The samples were analyzed as described in part A.

Table 2: Photoincorporation of Nucleotides into aFGF

nucleotide	app K_d (μM)	85–90% protection (μM)	% modified (min)
8N$_3$-ATP	2–2.5	200	9
2N$_3$-ATP	40–50	400	6
8N$_3$-GTP	3–3.5	200	7
8N$_3$-Ap$_4$A	2–3	300	19

completely inhibited photoincorporation under these conditions. Total protection by heparin was observed at the lowest molar ratio of heparin to aFGF examined (0.25).

The probe [^{32}P]-8N$_3$-ATP was chosen to attempt physical localization of the aFGF polyanion binding site. To this end, aFGF was photolabeled with 8N$_3$-ATP, precipitated by PCA and digested with trypsin. This material was fractionated by immobilized-Al^{3+} chromatography as described previously (Chavan et al., 1992; Salvucci et al., 1992; Shoemaker & Haley, 1993). A single radioactive peak (fractions 22–24) was obtained (Figure 7A), which was further separated by reverse phase HPLC (Figure 7B). The two most intensely labeled peaks at 34 and 41 min were subjected to amino acid sequence analysis in an attempt to determine the sites of photoinsertion. These results are summarized in Table 3.

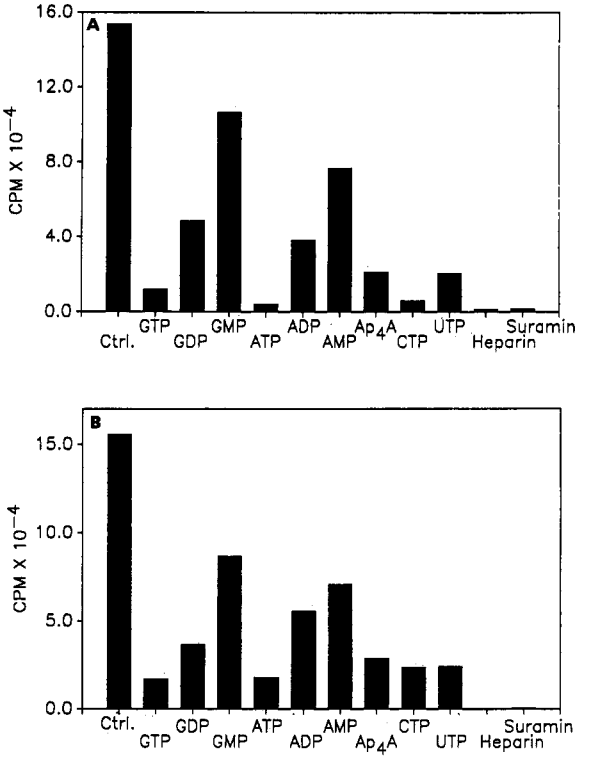

FIGURE 6: (A) Protection of photoinsertion of [γ-^{32}P]-8N$_3$-ATP into aFGF with various nucleotides. aFGF (1.0 μg) was incubated in a 30-μL final volume of photolysis buffer with a 100 μM concentration of the indicated competitor for 1 min at 4 °C followed by 5.0 μM probe for 30 s at 4 °C and photolysis for 30 s at 4 °C. The samples were analyzed as described in Figure 5A. (B) Protection of photoinsertion of [γ-^{32}P]-8N$_3$-GTP into aFGF with various nucleotides. aFGF (1.0 μg) was incubated in a 30-μL final volume of photolysis buffer with 100 μM competitors for 1 min at 4 °C followed by 5.0 μM probe for 30 s at 4 °C and photolysis for 30 s at 4 °C. The samples were analyzed as described in Figure 5A.

The peak at 34 min contained two sequences corresponding to aFGF peptides 1–11 and 13–23. While there was no immediate evidence of a labeled residue in the first sequence (although see Y8 below), in the second, glycine 20 was not detected and histidine 21 was present in only trace amounts, making them both candidates for modified amino acids. Note that trypsin failed to cleave as expected at the double basic site lysine 9/lysine 10, consistent with some modification in this region. The second peak contained three sequences. The first peptide started at serine 58 with significant material detected to asparagine 80. The only candidate for photoinsertion in this long sequence was threonine 61, which was not detected despite its potential presence in only the fourth sequencing cycle. A very small amount of the sequence 123–137 was found in which glycine 126 was absent, but if this residue was labeled, sequencing would be expected to stop at this position. We therefore feel that Gly 126 can only be tentatively suggested as a possible candidate for the labeled residue in this peptide. Rather, the drop in yield of His 124, which was confirmed in repeat experiments, suggests that this residue more probably contains the majority of the label. Finally, the short sequence of residues 113–118 was present in which the serine expected at position 116 was not seen. In summary, residues Gly 20, His 21, Thr 61, His 124, and Ser 116 all appear to be potential sites for photoinsertion of 8N$_3$-ATP into aFGF, with Gly 126 a more suspect candidate.

To further explore the location of potential labeled residues, photolabeled aFGF was also digested with chymotrypsin and fractionated with immobilized-Al^{3+} chromatography. A single radioactive peak was seen at 33 min, which was repurified on

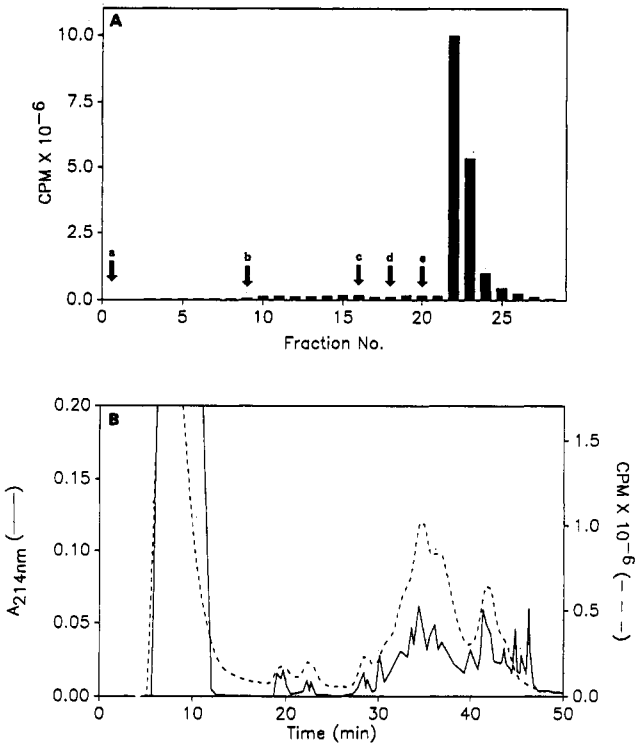

FIGURE 7: Isolation of [γ-^{32}P]-8N_3-ATP photolabeled tryptic peptides of aFGF. aFGF (500 μg) was photolyzed twice with probe and digested with trypsin as described in the experimental procedures. (A) Radioactivity elution profile for immobilized Al^{3+} chromatography. The Al^{3+} affinity resin was prepared as described in the experimental procedures. The digested aFGF was diluted with buffer A and (a) loaded onto the resin, (b) washed with buffer A, (c) washed with buffer A containing 0.5M NaCl, (d) washed with buffer A, and (e) washed with buffer A containing 10 mM K_2PO_4, pH 8.0. The radioactivity in fractions collected (~1.5 mL) was determined by Cerenkov counting. (B) Reverse phase HPLC profile of the purification of photolabeled peptides. Fractions 22–24 from part A were pooled, concentrated, and purified by reverse phase HPLC on an Aquapore RP300 C8 column employing a gradient of 0% B at 0–5 min and 100% B at 65 min at 0.5 mL/min (solvent A, 0.1% TFA; solvent B, 70% acetonitrile, 0.1% TFA). The radioactivity in fractions collected (0.5 mL) was determined by Cerenkov counting. Fractions 35 and 42 were subjected to amino acid sequence analysis on an Applied Biosystems 477A protein sequenator.

a C8 column. The single peak obtained in the second fractionation was then sequenced, and four sequences were observed (Table 4). In the first peptide (2–15), tyrosine 8 was reproducibly present in only trace amounts. Note that a significant drop in yield was also observed in this residue in the trypsin experiment (Table 3). In the second peptide (16–22), histidine 21 was not detected as seen in the trypsin digestion experiments. In a third peptide (75–86), the yield of proline 79 was low, but this was not confirmed when the protein was relabeled and digested and the peptides were reisolated and sequenced. In the final peptide identified (112–125), low yields were seen for residues lysine 113, serine 116, histidine 124, and arginines 119 and 122. In the repeat experiment, lysine 112 was labeled instead of 113 and serine 116 was not detectable, but the rest of the basic residues were only partially decreased in yield. It should also be noted that chymotrypsin failed to produce the expected cleavage at phenylalanines 7 and 85. Thus, chymotrypsin cleavage of 8N_3-ATP-labeled aFGF suggests possible labeling sites at histidine 21 and serine 116 as seen in the trypsin studies, as well as potential additional sites at tyrosine 8 and basic residues Lys 112, Lys 113, Arg 119, Arg 122, and His 124.

Acidic FGF photolabeled with 8N_3-ATP was also fractionated by heparin affinity chromatography, and a typical

Table 3: Sequence Analysis of Photolabeled aFGF Peptides Produced by Trypsin Digestion[a] (PTH-Amino Acids [pmol])

cycle	34 min		41 min		
1	^{1}F (55)	^{13}L (64)	^{58}S (82)	^{123}T (18)	^{113}K (25)
2	N (43)	L (51)	T (100)	H (5)	N (76)
3	L (60)	Y (36)	E (99)	Y (15)	G (72)
4	P (74)	C (nd)	T (nd)	G (nd)	S (nd)
5	P (65)	S (25)	G (118)	Q (10)	C (nd)
6	G (5)	N (32)	Q (88)	K (15)	^{118}K (15)
7	N (32)	G (55)	Y (74)	A (5)	
8	Y (12)	G (nd)	L (101)	I (5)	
9	K (17)	H (3)	A (74)	L (30)	
10	K (15)	F (18)	M (47)	F (5)	
11	^{11}P (9)	^{23}L (19)	D (43)	L (6)	
12			T (32)	P (3)	
13			D (50)	L (34)	
14			G (25)	P (4)	
15			L (25)	^{137}V (2)	
16			L (48)		
17			Y (27)		
18			G (16)		
19			S (9)		
20			Q (13)		
21			T (8)		
22			P (4)		
23			^{80}N (7)		

[a] The abbreviation nd denotes that the indicated amino acid was not detected. Cysteine was not detectable by this analysis. The superscripts indicate the position of the residues in the sequence of the form of human aFGF employed in these studies (Volkin et al., 1993).

Table 4: Sequence Analysis of Photolabeled aFGF Peptides Produced by Chymotrypsin Digestion[a] (PTH-Amino Acids [pmol])

cycle				
1	^{2}N (26)	^{16}C (nd)	^{75}G (44)	^{112}K (35)[b]
2	L (58)	S (18)	S (18)	K (4)
3	P (40)	N (18)	Q (27)	N (18)
4	P (30)	G (30)	T (27)	G (30)
5	G (29)	G (29)	P (6)[c]	S (8)[d]
6	N (44)	H (nd)	N (44)	C (nd)
7	Y (1)	^{22}F (5)	E (16)	K (10)
8	K (11)		E (12)	R (2)
9	K (8)		C (nd)	G (13)
10	P (15)		L (1)	P (15)
11	K (5)		F (2)	R (1)
12	L (8)		^{86}L (8)	T (12)
13	L (8)			H (nd)
14	^{15}Y (7)			^{125}Y (7)

[a] the abbreviation nd denotes that the indicated amino acid was not detected. Cysteine was not detectable by this analysis. The superscripts indicate the position of the residues in the sequence of the form of human aFGF employed in these studies (Volkin et al., 1993). [b] In a second experiment, ^{112}K rather than ^{113}K was low. [c] ^{79}P was not labeled in a repeat of this experiment. [d] ^{116}S was completely undetected in a second experiment.

chromatogram is shown in Figure 8. Native, unlabeled aFGF as well as the growth factor exposed to UV light in the absence of nucleotides elutes at a sodium chloride concentration of 1.35 M. In contrast, the photolabeled protein elutes as three distinct peaks between 0.3 and 0.45 M salt. The spectrum of each of these species is shown in the inset to Figure 8. Unlabeled aFGF possesses a typical protein near-UV spectrum with a peak near 280 nm. The photolabeled samples all display spectra dominated by the bound nucleotide with maxima between 260 and 270 nm and variable intensities. This suggests that at least three unique nucleotide–aFGF complexes are formed in these 8N_3-ATP photolabeling experiments. Although sufficient quantities of each complex were not obtained for further physical characterization, it was possible to examine their individual mitogenic activity, and the results are shown in Figure 9. These measurements were conducted in the

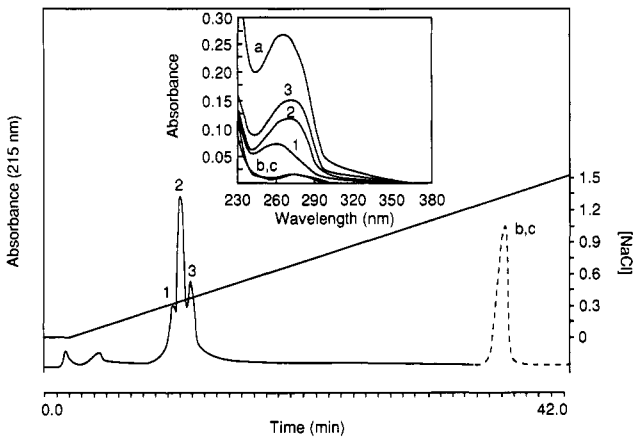

FIGURE 8: Heparin affinity chromatography of $8N_3$-ATP-labeled aFGF (solid line). The NaCl gradient used to elute the protein is shown also. The elution position of aFGF itself as well as aFGF exposed to UV light in the absence of $8N_3$-ATP is represented by the dashed line and the symbols b and c. The inset shows the near-UV spectra of peaks 1, 2, and 3 as well as that of the unlabeled protein (b and c) and the unfractionated $8N_3$-ATP-labeled aFGF that was applied to the column (a). All spectra were obtained at a protein concentration of approximately 20 μg/mL in 25 mM Tris, 0.4 M NaCl buffer at pH 7.5.

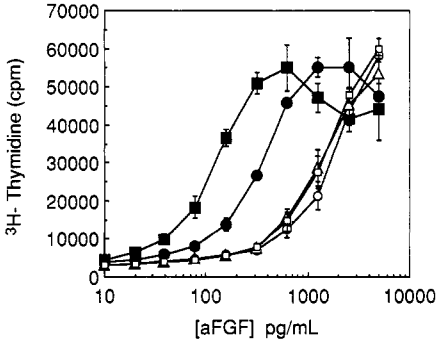

FIGURE 9: Effect of $8N_3$-ATP photolabeling of aFGF on the mitogenic activity of the growth factor. Mouse fibroblast 3T3 cells were treated with varying amounts of aFGF in the presence of 0.5 mg/mL heparin, and the resulting stimulation was measured by the incorporation of tritiated thymidine: (■) aFGF; (●) unfractionated $8N_3$-ATP-labeled aFGF; (□, △, ○) peaks 1, 2, and 3 (respectively) of purified $8N_3$-ATP-labeled aFGF eluted from heparin affinity column as described in Figure 8.

presence of an excess of heparin to test the effect of covalent modification of aFGF under maximum stimulatory conditions. Each of the three photolabeled complexes was approximately 20-fold less effective at inducing mitosis in 3T3 cells than native, unlabeled protein. Thus, each of the isolated, photolabeled proteins possesses mitogenic activity similar to that of the growth factor in the absence of polyanions, despite the presence of an excess of heparin in the culture medium. Unfractionated, photolabeled aFGF was intermediate in effectiveness, but these samples contain a significant amount of noncovalently bound nucleotide which would be displaced by heparin resulting in a significant portion of fully active aFGF–heparin complexes.

DISCUSSION

This work clearly establishes that nucleotides have the ability to bind and stabilize aFGF. This interaction appears to be primarily a function of the phosphate groups since increasing the degree of phosphorylation of all nucleosides examined produces a corresponding increase in the ability of aFGF to bind the compound. This is seen in studies of both the effects of nucleotides on the stability of aFGF (as monitored by aggregation, CD, and fluorescence) and their ability to photolabel the growth factor. In fact, tripolyphosphate is an even more effective stabilizer of aFGF than any of the nucleotide triphosphates, suggesting that the presence of the sugar/base moiety may actually decrease the effectiveness of the polyanionic portion of the molecules as ligands for aFGF (Table 1). The antagonistic effect of the sugar/base is also clearly seen in the diadenosine compounds in which one to two additional phosphates are necessary to offset the presence of the two nucleotides. The particular base seems less important, however, since the different NTPs all have similar effects, although modification of the base (e.g., compare photolabeling by 8- and $2N_3$-ATP) can have a significant effect.

A second conclusion from this work is that the nucleotides (and polyphosphates) bind to the previously recognized polyanion binding site on aFGF. The location of this region on the surface of aFGF has recently been identified from crystal structures of bovine aFGF in which the polyanions sucrose octasulfate (Zhu et al., 1993) and naphthalene trisulfonate are bound (Zhu, 1993). This work has identified Asn 18, Lys 112, Lys 113, Asn 114, Arg 116 (Ser in human aFGF), Lys 118, Arg 122, Gln 127, and Lys 128 as residues in direct contact with negatively charged portions of the polyanions. These nine residues form a distinctive, large patch of positive charge density on the surface of the growth factor. Both sucrose octasulfate (Zhu et al., 1993) and naphthalene trisulfonate (Zhu, 1993), as well as various small anions (Zhu et al., 1991), bind in well-defined orientations within this region. Nevertheless, this polyanion binding site appears to be very promiscuous with many polyanionic substances able to interact with varying degrees of affinity in this region (Tsai et al., 1993; Volkin et al., 1993). This probably reflects both the extent of this region on the surface of aFGF as well as the complexity of the microenvironment of this site, which presumably offers a plethora of potential multiple contact geometries to negatively charged ligands. Nucleotides and polyphosphates seem to be primarily binding to this particular polyanion binding site since there is efficient competition for this binding by heparin, sucrose octasulfate, and other polyanions, although as discussed below this does not exclude the existence of additional polyanion binding regions. Furthermore, the reactivity of the aFGF thiol near this site is also perturbed by the polyphosphates and nucleotides as previously seen with other polyanions (Volkin et al., 1993).

As shown in Figure 10, eight of the residues that are candidates for photolabeling by $8N_3$-ATP (Gly 20, His 21, Lys 112, Lys 113, Ser 116, Arg 119, Arg 122, His 124) are located around the perimeter of the consensus polyanion binding region. Since neither a single residue nor a tightly clustered group of residues is labeled, this suggests that $8N_3$-ATP is able to bind in a number of different orientations in this region. This is entirely consistent with the nonspecific nature of this binding site and the fact that at least three different forms of photolabeled complexes can be resolved by heparin affinity chromatography (Figure 8). A fifth residue (Thr 61), however, also appears to be photolabeled in the trypsin studies, and this moiety is a significant distance from this region. Although a peptide containing this residue was not found after chymotrypsin digestion, a significant reduction in yield at this position was reproducible in the trypsin experiments. Threonine 61 is located at the edge of another positively charged rich region comprising Lys 12, Arg 35, Arg 37, His 41, and Lys 57 (Zhu et al., 1991; not illustrated).

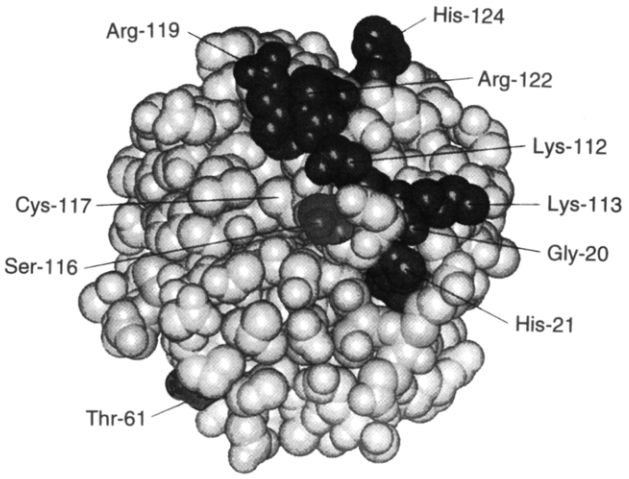

FIGURE 10: Space-filling model of human aFGF illustrating the residues potentially photolabeled by aFGF. The origin of this model is described in Volkin et al. (1993). Candidate photolabeled amino acids are indicated in black with the individual residues identified. Cys 117 is also identified for reference purposes.

A peptide containing the latter four residues (35–57) has previously been shown to compete for binding of derivatized heparin to aFGF (Burgess, 1992). This same region has been implicated in receptor binding (Baird et al., 1988; Yu et al., 1992) and has been proposed to be part of an aFGF dimerization interface in crystals (Zhu, 1993; Zhu et al., 1993). Thus, the presence of a second or dramatically extended polyanion binding site is hinted by this work, but these results may simply be explained by the low specificity of polyanion binding. Furthermore, no evidence for such a site has yet been found by X-ray crystallography. Indeed, the positively charged residues in this region are much more widely spaced than those seen in the consensus polyanion binding site. It follows that small anions (e.g., sulfate, phosphate, iridium hexachloride, selenate) and polyanions (napthalene trisulfonate) might not be capable of bridging these more widely spaced residues. In contrast, the polysulfate moieties might be able to extend across the surface to more easily interact with several of the Lys 12, Arg 35, Arg 37, His 41, and Lys 57 side chains. The existence of this second polyanion binding site, however, will clearly require additional evidence to establish its presence on aFGF. It is, however, consistent with the ability of large, symmetrical polyanions such as suramin to cross-link aFGF to an extent much greater than dimeric oligomers (Middaugh et al., 1992), and the observation that molar excesses of heparin decrease the unfolding rate of the protein (Burke et al., 1993). Evidence for labeling of Tyr 8 was also found in the chymotrypsin experiments as well as supported by lack of trypsin cleavage in this region, but the flexibility of the N-terminal peptide does not permit this site to be visualized in crystal structures, making its location currently uncertain.

On the basis of the evidence of these studies, can we classify aFGF as a nucleotide binding protein? In a literal sense, the answer could be yes since aFGF clearly binds nucleotides with high affinity and they can be displaced by related structures. Although aFGF does not contain any of the exact consensus elements described for well-established nucleotide binding proteins (GXXXXGK, DXXG, NKXD) (Moller & Amons, 1985; Dever et al., 1987), it does possess a number of short sequences which are reminiscent of these regions (i.e., ^{29}GTVD^{32}, ^{49}ESVG^{52}, ^{68}DTDG^{71}, ^{119}RGPRTHYG^{126}), although consensus spacing of these elements is also absent. More strictly, however, the answer must be no since a wide variety of other highly polyanionic substances are also capable of competing for binding. Furthermore, the absence of orientational specificity by the bound nucleotide as evidenced by the dispersed labeling pattern is more consistent with nonspecific binding. It should be noted, however, that polyanions such as heparin can compete for ATP in known nucleotide binding proteins such as ATPases (Cruz & Dietrich, 1967; Tersariol et al., 1992). Thus, a combination of the identity of the ligands present and their relative amounts and affinity for the aFGF polyanion binding site should determine the nature of any natural aFGF–polyanion complexes found *in vivo*. As such, the presence of high intracellular concentrations of nucleotide triphosphates (especially ATP) does make this a candidate for a biological aFGF ligand, although this need not imply any functional importance to ATP as an energy source *per se*. Although physiological roles for diadenosine compounds have been proposed (Zamecnik, 1983; Andersson, 1989), their lower intracellular concentrations make them less attractive possibilities. The more highly phosphorylated inositols also bind tightly to aFGF (Volkin et al., 1993), as well as undergo significant changes in their intracellular levels (Bunce et al., 1993; Guse et al., 1993; Menniti et al., 1993). These compounds can also be present at sufficiently high concentrations (1–100 μM) that a biological role for them in aFGF stabilization should also be considered. Despite the potential lack of specificity of the NTPs and IHPs, they could have actual effector functions if their aFGF binding affinity and concentrations are such that they are the primary binding polyanions present in cells. For example, a drop in polyanion concentration at physiological temperature could produce translocation competent (structurally disrupted, e.g., molten globule) aFGF (Wiedlocha et al., 1992; Mach et al., 1993a), which could be transported out of cells in perhaps a chaperone dependent manner. Conversely, elevated levels of NTPs or IHPs could inhibit aFGF release. We have as of yet, however, been unable to find any experimental evidence in support of such mechanisms. Preliminary studies suggest that aFGF can be covalently modified by ATP in the absence of extrinsic enzymatic activity providing another way in which polyanions could alter the activity of aFGF. These possibilities are under active investigation.

REFERENCES

Andersson, M. (1989) *Int. J. Biochem. 21*, 707–714.
Baird, A., Schubert, D., Ling, N., & Guillemin, R. (1988) *Proc. Natl. Acad. Sci. U.S.A. 85*, 2324–2328.
Bunce, C. M., French, P. J., Allen, P., Mountford, J. C., Moor, B., Greaves, M. F., Michell, R. H., & Brown, G. (1993) *Biochem. J. 289*, 667–673.
Burgess, W. H. (1992) *Ann. N.Y. Acad. Sci. 638*, 89–97.
Burke, C. J., Volkin, D. B., Mach, H., & Middaugh, C. R. (1993) *Biochemistry 32*, 6419–6426.
Chavan, A. J., Nemoto, Y., Narumiya, S., Kozaki, S., & Haley, B. E. (1992) *J. Biol. Chem. 267*, 14866–14870.
Copeland, R. A., Ji, H., Halfpenny, A. J., Williams, R. W., Thompson, K. C., Herber, W. K., Thomas, K. A., Bruner, M. W., Ryan, J. A., Marquis-Omer, D., Sanyal, G., Sitrin, R. D., Yamazaki, S., & Middaugh, C. R. (1991) *Arch. Biochem. Biophys. 289*, 53–61.
Cruz, W. O., & Dietrich, C. P. (1967) *Proc. Soc. Exp. Biol. Med. 126*, 420–426.
Czarnecki, J., Geahlen, R. T., & Haley, B. E. (1979) *Methods Enzymol. 56*, 642–653.
Dabora, J. M., Sanyal, G., & Middaugh, C. R. (1991) *J. Biol. Chem. 266*, 23637–23640.

Dever, T. E., Glynias, M. J., & Merrick, W. C. (1987) *Proc. Natl. Acad. Sci. U.S.A. 84*, 1814–1818.
Guse, A. H., Greiner, E., Emmrich, F., & Brand, K. (1993) *J. Biol. Chem. 268*, 7129–7133.
Haley, B. E. (1991) *Methods Enzymol. 200*, 477–487.
Lehninger, A. L. (1982) *Principles of Biochemistry*, p 373, Worth Publishers, New York.
Linemeyer, D. L., Kelly, L. J., Menke, J. G., Gimenez-Gallego, G., DeSalvo, J., & Thomas, K. A. (1987) *Biotechnology 5*, 960–965.
Mach, H., Ryan, J. A., Burke, C. J., Volkin, D. B., & Middaugh, C. R. (1993a) *Biochemistry 32*, 7703–7711.
Mach, H., Volkin, D. B., Burke, C. J., Middaugh, C. R., Linhardt, R. J., Fromm, J. R., Loganathan, D., & Mattsson, L. (1993b) *Biochemistry 32*, 5480–5489.
Menniti, F. S., Oliver, K. G., Putney, J. W., Jr., & Shears, S. B. (1993) *Trends Biochem. Sci. 18*, 53–56.
Michelson, A. M. (1964) *Biochim. Biophys. Acta 91*, 1–13.
Middaugh, C. R., Mach, H., Burke, C. J., Volkin, D. B., Dabora, J. M., Tsai, P. K., Bruner, M. W., Ryan, J. A., & Marfia, K. E. (1992) *Biochemistry 31*, 9016–9024.
Moller, W., & Amons, R. (1985) *FEBS Lett. 186*, 1–7.
Ornitz, D. M., Yayon, A., Flanagan, J. G., Svahn, C. M., Levi, E., & Leder, P. (1992) *Mol. Cell. Biol. 12*, 240–247.
Salvucci, M. E., Chavan, A. J., & Haley, B. E. (1992) *Biochemistry 31*, 4479–4487.
Shoemaker, M. T., & Haley, B. E. (1993) *Biochemistry 32*, 1883–1890.
Tersariol, I. L. S., Dietrich, C. P., & Nader, H. B. (1992) *Thrombosis Res. 68*, 247–258.
Tsai, P. K., Volkin, D. B., Dabora, J. M., Thompson, K. C., Bruner, M. W., Gress, J. O., Matuszewska, B., Keogan, M., Bondi, J. V., & Middaugh, C. R. (1993) *Pharm. Res. 10*, 649–659.
Vlodavsky, I., Fuks, Z., Ishai-Michaeli, R., Bashkin, P., Levi, E., Korner, G., Bar-Shavit, R., & Klagsbrun, M. (1991) *J. Cell. Biochem. 45*, 167–176.
Volkin, D. B., Tsai, P. K., Dabora, J. M., Gress, J. O., Burke, C. J., Linhardt, R. J., & Middaugh, C. R. (1993) *Arch. Biochem. Biophys. 300*, 30–41.
Wiedlocha, A., Madshus, H., Mach, H., Middaugh, C. R., & Olsnes, S. (1992) *EMBO J. 11*, 4835–4842.
Yu, Y.-L., Kha, H., Golden, J. A., Migchielsen, A. J. J., Goetzl, E. J., & Turck, C. W. (1992) *J. Exp. Med. 175*, 1073–1080.
Zamecnik, P. (1983) *Anal. Biochem. 134*, 1–10.
Zhu, X. (1993) Structure-function Studies of Fibroblast Growth Factors (FGFs), Ph.D. Thesis, California Institute of Technology.
Zhu, X., Komiya, H., Chirino, A., Faham, S., Fox, G. M., Arakawa, T., Hsu, B. T., & Rees, D. C. (1991) *Science 251*, 90–93.
Zhu, X., Hsu, B. T., & Rees, D. C. (1993) *Structure 1*, 27–34.